RESONANCE COMPENSATION AT THE CERN PS BOOSTER AIDED BY BAYESIAN OPTIMIZATION AND BOBYQA

C. E. Gonzalez-Ortiz*, Michigan State University, East Lansing, USA

R. Ainsworth, Fermilab, Batavia, USA

F. Asvesta, T. Prebibaj, CERN, Geneva, Switzerland

Abstract

The CERN Proton Synchrotron Booster (PSB) operation involves the crossing of multiple resonance lines in the tune diagram. Loss maps from dynamic tune scans are a helpful way to visualize and quantify the strength of such resonances. Sextupole and octupole correctors can be used in order to partially or fully compensate multiple resonance lines, i.e., third and fourth order lines. The following work explores the application of advanced optimization algorithms such as Bayesian Optimization and Bound Optimization By Quadratic Approximation (BOBYQA) in order to compensate these resonance lines with available correctors.

INTRODUCTION

The Proton Synchrotron Booster (PSB) is the first circular accelerator in the CERN accelerator complex that ultimately leads to the LHC. Following the successful implementation of the LHC Injectors Upgrade (LIU) [1], the PSB receives H^- ion beam from the Linac4 at an energy of 160 MeV. Interestingly, the PSB is not just one ring but four identical synchrotron rings stacked on each other. This design counteracts the space charge effects, which are the largest in low-energy machines. Once the ion beam enters the PSB rings, the electrons are stripped off through a charge-exchange process with a carbon foil, and a proton beam is achieved [2]. The proton beam is then accelerated from an energy of 160 MeV to 2 GeV. Each ring extracts one bunch and is injected in different buckets into the Proton Synchrotron (PS). This description is true for LHC-type beams. Nevertheless, the PSB can also operate on other modes to feed protons to other customers such as its highest-intensity user—ISOLDE (Isotope mass Separator On-Line facility) [3]—or fixed-target experiments such as SFTPRO [4].

Figure 1 illustrates the tune diagram dynamics that the LHC-type beam undergoes at the PS Booster [3, 5, 6]. The beam gets injected at an energy of 160 MeV. At this low energy, the tune footprint is large enough that the spread can reach up to 0.5, i.e., $\Delta Q_u \approx -0.5$. The nominal injection tunes are around $Q_x = 4.40$ and $Q_y = 4.45$, in order to accommodate the footprint between the integer resonance lines $Q_u = 4.0$ and the half-integer line $2Q_y = 9$. As the beam is accelerated, the quadrupoles are ramped up to match the increasing beam rigidity, but, additionally, a tune ramp is introduced to move the shrinking footprint to a less resonance-populated area in the tune diagram. The nominal extraction tunes are around $Q_x = 4.17$ and $Q_y = 4.23$. At
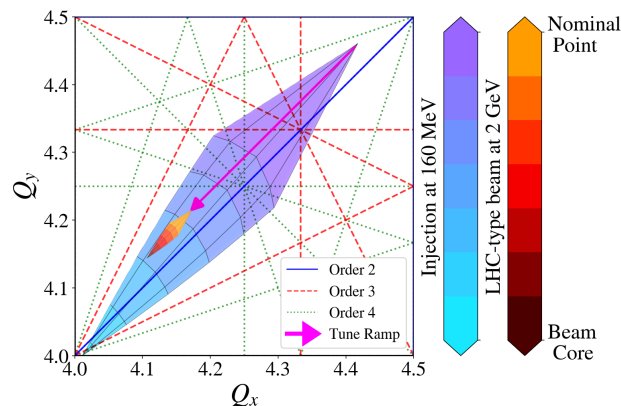
* gonza839@msu.edu

Figure 1: Operational tune footprint for PSB beam at injection (cool color map) and footprint after the beam has been accelerated to 2 GeV (warm color map). During acceleration, there is a tune ramp illustrated with the fuchsia arrow.

extraction, the beam tune footprint has shrunk by a factor of $(\gamma_L^3 \beta_L^2)$. At extraction, the footprint is smaller than 0.05, i.e., $|\Delta Q_u| \lesssim 0.05$.

The objective of the following work is to minimize the losses during the PS Booster's operational cycle, as explained in Fig. 1. The losses during the cycle come from particles falling on top of third-order and fourth-order resonance lines. These experiments explore the use of advanced optimization algorithms to compensate for multiple resonance lines simultaneously.

EXPERIMENTAL SETUP

The experimental setup introduced in the PS Booster involved several steps to find the optimal compensation currents. First, a low-brightness beam was injected into every ring at an energy of 160 MeV. Energy is not ramped up for this configuration, and the machine stays at a flat bottom. Second, a tune ramp was programmed into the quadrupoles in the ring in order to go from initial tunes of $Q_x = 4.40$ and $Q_y = 4.45$ to a final setting of $Q_x = 4.17$ and $Q_y = 4.23$. This particular setting was introduced to mimic the operational tune ramp of the LHC-type beam. The start of this tune ramp occurs within $t_0 = 300$ ms of the start of the cycle and ends at $t_f = 600$ ms, i.e., all of this occurs within a 300 ms time window. This window corresponds to approximately 300000 turns of the beam inside the PSB and interacting with the resonances—increasing the sensitivity of the protons to the resonances. During this time window,

Table 1: List of elements (optimization actors) in the PS Booster at CERN used for resonance compensation optimization as present in all four PS Booster rings.

| Actor	Name	Type
1	XN04L1	Normal Sextupole
2	XN06L1	Normal Sextupole
3	XN09L1	Normal Sextupole
4	XN012L1	Normal Sextupole
5	XN0311L1	Normal Sextupole
6	XN0816L1	Normal Sextupole
7	ON0311L1	Normal Octupole
8	ON0816L1	Normal Octupole
9	XSK2L4	Skew Sextupole
10	XSK4L1	Skew Sextupole
11	XSK6L4	Skew Sextupole

Figure 2: Normalized beam current plots for the Bayesian Optimization method done at Ring 1.
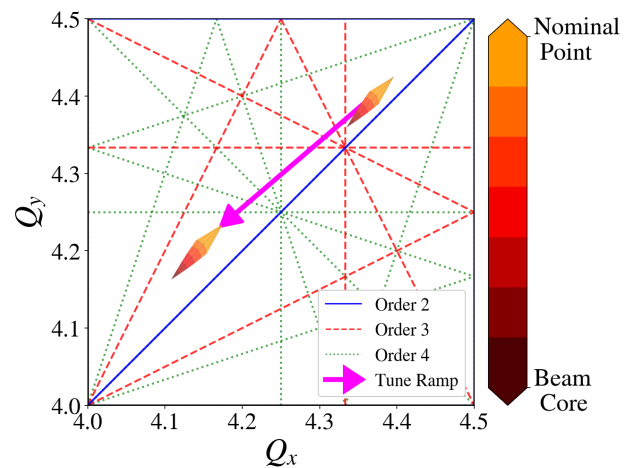

Figure 3: Experimental setup of the tune diagram dynamics for optimizing resonance compensation used in the PS Booster.

the beam loss is measured by comparing the beam current at the end of the window to the initial value of the beam current. The currents fed to the corrector magnets remain constant during this measurement.

While monitoring the beam loss, the corrector magnets used for compensation are varied every cycle according to the optimization algorithm. Table 1 summarizes the 11 elements used for resonance compensation for this work. Out of these elements, there are 6 normal sextupoles, 3 skew sextupoles, and 2 normal octupoles. Before the tune ramp, most actors show currents at or near zero. As preparation for the tune ramp, the magnets are powered to the set values—per the optimizer calculation. During the tune ramp, they are set to a constant value and powered off once the cycle is finished. These magnets were varied for each ring, and each ring had its independent optimization run. Theoretically, in order to fully correct eight resonance lines, one needs at least 16 correctors. Nevertheless, this work aimed to find a solution to this over-constrained problem through advanced optimization algorithms.

The two optimization algorithms used were Bayesian Optimization and BOBYQA (Bound Optimization BY Quadratic Approximation) [7–9]. In order to implement these algorithms, the special application GeOFF (Generic Optimization Frontend and Framework) was used [10]. This graphical application is designed to facilitate numerical optimization through various algorithms and reinforcement learning on CERN accelerators. It incorporates programmable interfaces that can be used to specify the hyperparameters of the optimization algorithms.

Figure 2 shows an example of the evolution of the objective function during a Bayesian optimization procedure. In this case, the objective function is the normalized beam loss after the tune ramp illustrated by Fig. 3. It can be seen how the Bayesian optimizer finds solutions that effectively cancel out the beam loss from crossing the resonances. Nevertheless, given that this optimizer is built to find a global minimum, it will keep sampling other regions to ensure the
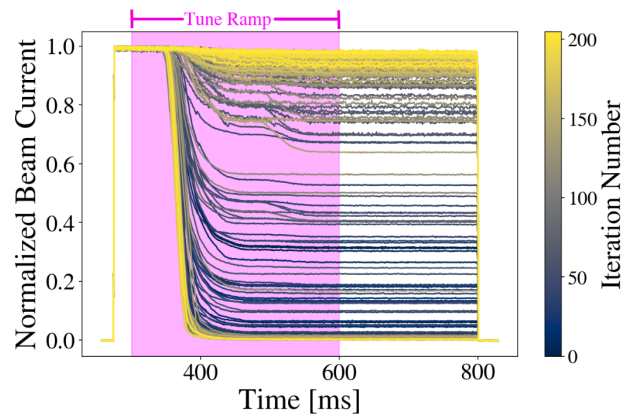
best solution is not a local minimum. The color map of Fig. 2 shows how for some of these cases, the optimizer prioritizes exploration and drifts to some unknown region where the losses are high. For these cases, the underlying Gaussian process will learn that there is no worth in exploring these regions. Ultimately, the configuration with the least relative beam loss—the best configuration—is saved and kept as the optimum solution.

On the other hand, Fig. 4 shows the explicit steps of each actor versus the number of iterations. Additionally, the top plot shows the trend of the objective function (relative beam loss) as the number of iterations increases. There are significant oscillations in the relative beam loss values, especially at the beginning, but a general trend towards minimization as the algorithm progresses through iterations. The early iterations reflect the exploration phase. BO is sampling points that give a broad understanding of the objective function's landscape. As iterations progress, there is a trend toward certain regions in the parameter space. This trend indicates a shift from exploration to exploitation, where the algorithm samples more from areas it believes to be near the optimum.
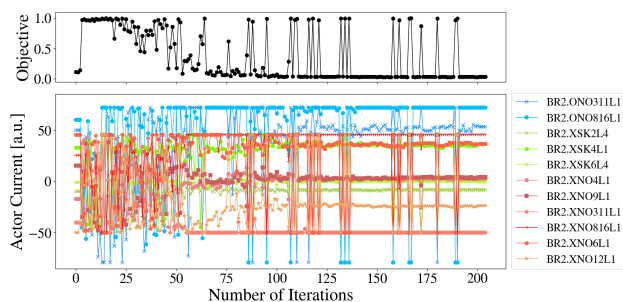
Figure 4: Summary for Bayesian optimization of resonance compensation applied to Ring 2 in the CERN PSB.

The narrowing of actor current variability suggests a reduction in uncertainty about the location of the minimum beam loss. The GP model is becoming more informed and better trained. At the end of the optimization instance, such as the one shown in Fig. 4, the configuration that gave the smallest relative beam loss is saved. GeOFF sets the default configuration of the correctors to these best values.

The corrector values for the best configurations are important to discuss from Fig. 4. It can be seen from Fig. 4 that some correctors land on the limit values, e.g., the limits for the normal sextupoles (XNO magnets) were [–50,50]. This behavior is especially apparent for the octupole correctors (ONO magnets), which have limits from –80 to 80, e.g., the magnet ONO816L1 is maxed out. These high currents indicate that the current corrector configuration is not sufficient to compensate the strength of the fourth-order resonances. Work is still ongoing to understand the octupole-like fields around the rings driving these resonances.

It is important to remember that implementing these types of algorithms with several actors efficiently requires the currents to be normalized between [0,1], so that all the data is on the same scale to improve the model performance. This procedure is done by GeOFF internally.

EXPERIMENTAL VERIFICATION

Loss Maps

Dynamic loss maps can be produced by mapping the beam losses in different tune directions and interpolating these maps. Reference [3] explains in detail the production of loss maps at the PSB. The whole point of the optimization algorithms explained in the last sections was to reduce the losses that show up in the loss map of the bare machine from Fig. 5.

Figure 6 shows a new loss map with the best configurations found for each ring using the Bayesian optimization procedure on LHC-type beam. When comparing both loss maps, it is clear that with these new configurations, the loss maps have been cleared out of losses in the region of interest. The immediate losses are decreased by nearly one order of magnitude in the region occupied by the tune ramp. In particular, these new configurations largely suppress the third-order resonances that dominated the losses in Fig 4.
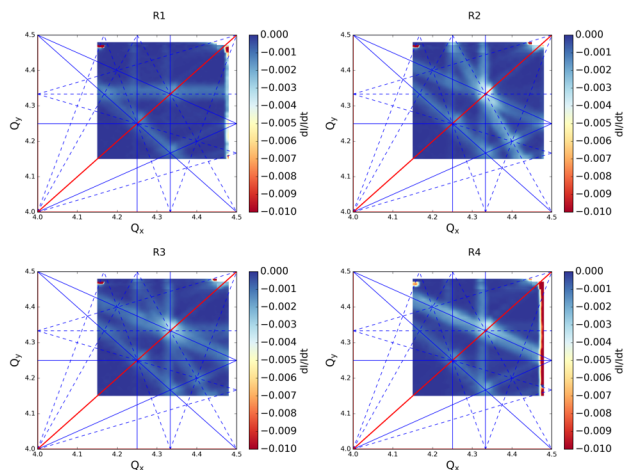

Figure 5: Dynamic loss maps for the bare machine of the four rings (R1, R2, R3, and R4) in the PS Booster. The plots are an average of scanning in 4 directions.
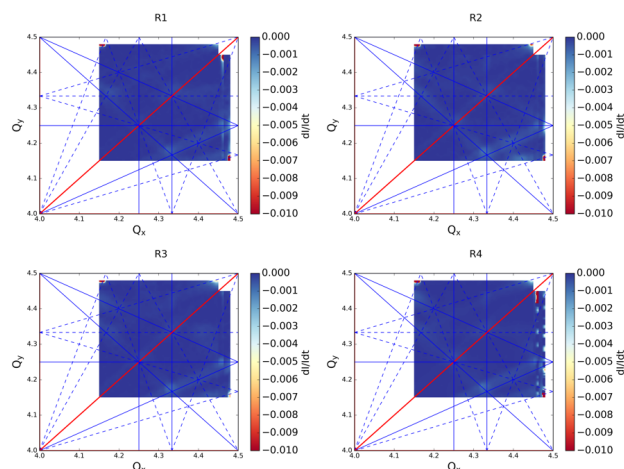

Figure 6: Dynamic loss maps for the four rings in the PS Booster with the best configuration from the Bayesian optimization of the resonance compensation. The plots are an average of scanning in 4 directions.

Nevertheless, some resonance lines are still visible in the loss maps in Fig. 5, e.g., $Q_x - 2Q_y = -4$. Given that these lines are not in the region of PSB operation, they are not of particular concern.

CONCLUSIONS

Nonlinear resonances pose critical limitations in the operations of the CERN PSB, both for high intensity and high brightness users. In particular, resonances up to 4th order have been observed and compensated for using magnet correctors. In order to simultaneously correct all the observed resonances, optimization techniques have been used giving excellent results on the injection energy plateau. Further studies are ongoing to implement an application based on the optimization techniques presented and to also address the correction along the cycle.

REFERENCES

[1] H. Damerau *et al.*, "LHC Injectors Upgrade, Technical Design Report". 2014. `doi:10.17181/CERN.7NHR.6HGC`. https://cds.cern.ch/record/1976692.

[2] W. Weterings *et al.*, "The new injection region of the CERN PS Booster", in *Proc. IPAC'19*, Melbourne, Australia, May 2019, pp. 2414-2417, `doi:10.18429/JACoW-IPAC2019-WEPMP039`

[3] Foteini Asvesta *et al.*, "Resonance Compensation for High Intensity and High Brightness Beams in the CERN PSB". in: JACoW HB 2021 (2022), pp. 40–45. `doi:10.18429/JACoW-HB2021-MOP06`. url: https://cds.cern.ch/record/2841816.

[4] A. Huschauer *et al.*, "Beam performance and operational efficiency at the CERN Proton Synchrotron", in in *Proc. IPAC'23*, Venice, Italy, May 2023, pp. 1671-1674, `doi:10.18429/JACoW-IPAC2023-TUPA158`

[5] F. Asvesta *et al.* "High Intensity Studies in the CERN Proton Synchrotron Booster", in *Proc. IPAC'22*, Bangkok, Thailand, July 2022, WEPOTK011, pp. 2056–2059. `doi:10.18429/JACoW-IPAC2022-WEPOTK011`

[6] S. Albright *et al.* "New Longitudinal Beam Production Methods in the CERN Proton Synchrotron Booster", in: *Proc. IPAC '21*, Campinas, SP, Brazil, May 2021, pp. 4130–4133. `doi:10.18429/JACoW-IPAC2021-THPAB183`

[7] M. Powell, "The BOBYQA Algorithm for Bound Constrained Optimization without Derivatives." *Technical Report*, Department of Applied Mathematics and Theoretical Physics, 2009.

[8] C. Cartis, J. Fiala, B. Marteau, and L. Roberts, "Improving the Flexibility and Robustness of Model-Based Derivative-Free Optimization Solvers", *ACM Transactions on Mathematical Software*, 45:3 (2019), pp. 32:1-32:41 [arXiv preprint: 1804.00154]

[9] C. Cartis, L. Roberts and O. Sheridan-Methven, "Escaping local minima with derivative-free methods: a numerical investigation, Optimization" (2021). [arXiv preprint: 1812.11343]

[10] Generic Optimization Frontend and Framework (GeOFF). https://gitlab.cern.ch/geoff/geoff-app.